Separation Science and Technology
Publication details, including instructions for authors and subscription information:
http://www.informaworld.com/smpp/title~content=t713708471

Treatment of Leather Plant Effluent by Membrane Separation Processes

S. K. Jain[a]; M. K. Purkait[a]; S. De[a]; P. K. Bhattacharya[b]
[a] Department of Chemical Engineering, Indian Institute of Technology, Kharagpur, India [b] Department of Chemical Engineering, Indian Institute of Technology, Kanpur, India

To cite this Article Jain, S. K. , Purkait, M. K. , De, S. and Bhattacharya, P. K.(2006) 'Treatment of Leather Plant Effluent by Membrane Separation Processes', Separation Science and Technology, 41: 15, 3329 — 3348
To link to this Article: DOI: 10.1080/01496390600915080
URL: http://dx.doi.org/10.1080/01496390600915080

Separation Science and Technology, 41: 3329–3348, 2006

ISSN 0149-6395 print/1520-5754 online
DOI: 10.1080/01496390600915080

Treatment of Leather Plant Effluent by Membrane Separation Processes

S. K. Jain, M. K. Purkait, and S. De
Department of Chemical Engineering, Indian Institute of Technology,
Kharagpur, India

P. K. Bhattacharya
Department of Chemical Engineering, Indian Institute of Technology,
Kanpur, India

Abstract: A scheme is proposed for the treatment of the leather plant effluent using membrane based separation processes. The effluent coming out from the various upstream units of the leather plant (except chrome tanning) are combined and a two step pressure driven membrane processes involving nanofiltration (NF) and reverse osmosis (RO) are adopted after a pretreatment consisting of gravity settling, coagulation, and cloth filtration. The entire membrane separation scheme is validated by conducting experiments under a continuous cross flow mode. A detailed parametric study for cross flow experiments is investigated to observe the effects of the operating conditions, i.e., the transmembrane pressure drop and the cross flow velocity on the permeate flux and quality for both NF and RO. Using a combination of osmotic pressure and solution diffusion model for both NF and RO, the effective osmotic pressure coefficient, solute diffusivity, and the solute permeability through the membrane are obtained by optimizing the experimental permeate flux and concentration (in terms of total dissolved solids) values for this complex industrial effluent. The BOD and COD values of the finally treated effluent are well within the permissible limits (in India).

Keywords: Leather plant effluent, membrane, nanofiltration, reverse osmosis, chemical oxygen demand, conductivity, total dissolved solids

Received 31 March 2006, Accepted 8 June 2006

Address correspondence to S. De, Department of Chemical Engineering, Indian Institute of Technology, Kharagpur, 721302, India. Tel.: +91-3222-283926; Fax: +91-3222-255303; E-mail: sde@che.iitkgp.ernet.in

INTRODUCTION

Increasing industrial density, human population, and use of the old and polluting technologies lead to increasing environmental pollution. Since the environmental protection has now become a global issue, a cleaner and greener technology is warranted for the abatement of the industrial pollution. The leather industry is one such highly polluting industry. Leather is a natural product like wool and is obtained from a variety of animals, like, cows, sheep, goats, etc. The transformation of the raw hide into leather requires various mechanical treatments and also a series of chemical treatments. Chemical processing is generally carried out using different chemicals; e.g., acids, alkalis, salts of sodium and chromium, dyes, etc. (1).

In India, the annual amount of hides and skins processed is about 70,000 tonnes resulting in 75,000 m^3 of the liquid effluent per day (2). Sodium chloride, sodium sulfide, lime, chromium, protein, fats, etc. are the major constituents (3). The effluent has a high biological oxygen demand (BOD) and chemical oxygen demand (COD). Small scale tanneries release the effluents from the "beam house" through a common header directly to the sewage/river stream.

Membrane based processes offer a cleaner technology in the treatment of various industrial processes for separation, purification, concentration, and fractionation of the solutes (4–7). Cassano et al. (8) presented a detailed conceptual possibility of various applications of the membrane based processes, e.g., microfiltration (MF), ultrafiltration (UF), nanofiltration (NF), and reverse osmosis (RO) on different effluent streams of the beam house. Application of NF to the effluent from the liming (9) and UF from the degreasing (10, 11) unit have been reported. The use of UF and RO to treat the soaking, deliming/bating, and pickling effluents are conceptualized (8). The treatment of the chromium rich tanning effluents using UF and NF is mostly studied (12–17) for the recovery and reuse of tanning chemicals. However, application of the membrane based processes to treat each of the "beam house" effluent becomes cost intensive.

Hence, it is envisaged that the combined effluents coming from all the "beam house" processes, namely, soaking, liming, fleshing, deliming, bating, pickling, and skin degreasing (just before the tanning step), may be treated by a two–step membrane based process (NF followed by RO) after proper pre-treatment (using gravity settling, coagulation, and coarse filtration). The performance criteria of these membrane processes are evaluated in terms of COD, BOD, conductivity, total dissolved solids, and the permeate flux of the treated effluent. The validity of the above scheme is tested in a continuous cross flow cell. It is envisaged that the retentate of both the membrane processes can be recycled to the gravity settling chamber for further processing and the final permeate of RO can be recycled back to the "beam house" for make up water and chemicals. The schematic of the treatment of the effluent is shown in Fig. 1. A detailed parametric study is

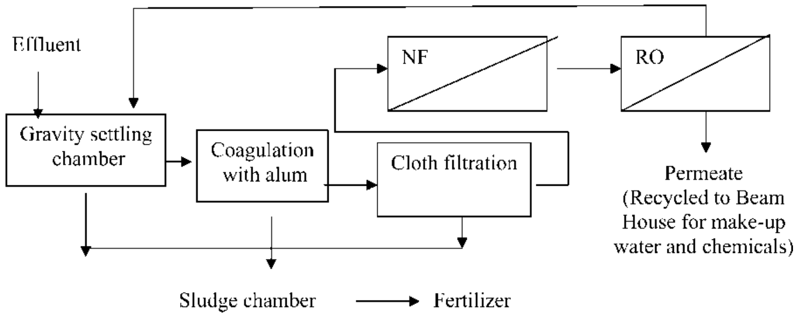

Figure 1. Proposed scheme for the treatment of effluent 1.

carried out in a continuous cross flow system by varying the cross flow rates and the operating pressures. An osmotic pressure model is used in combination of a solution diffusion model to determine the various process parameters, namely, effective osmotic pressure, solute diffusivity, and solute permeability through the membrane for this complex effluent, in case of NF as well as RO.

THEORY

Using the osmotic pressure model, the permeate flux is expressed as,

$$J = L_p(\Delta P - \Delta\pi) \tag{1}$$

The osmotic pressure difference across the membrane is given as,

$$\Delta\pi = \pi_m - \pi_p \tag{2}$$

where, π_m is the osmotic pressure at the membrane surface and π_p is that in the permeate stream. Being a colligative property, the osmotic pressure is related to the solute concentration through vant Hoff's relationship,

$$\pi = ac \tag{3}$$

where, the osmotic coefficient a is given as $a = RT/M$. Using Eqs. (1) to (3), the permeate flux is described as,

$$J = L_p[\Delta P - a(c_m - c_p)] \tag{4}$$

According to the stagnant film theory, the permeate flux is expressed in terms of mass transfer coefficient as,

$$J = k\ln\left(\frac{c_m - c_p}{c_0 - c_p}\right) \tag{5}$$

Combining Eqs. (4) to (5), the following expression is obtained,

$$J_w^0\left[1-\alpha\left(c_m-c_p\right)\right]=k\ln\left(\frac{c_m-c_p}{c_0-c_p}\right) \tag{6}$$

where, $\alpha = a/\Delta P$ and $J_w^0 = L_p\Delta P$.

According to solution diffusion model, the solute flux through the membrane is proportional to the concentration difference across the membrane surface. Therefore, the following equation is obtained,

$$Jc_p = B\left(c_m - c_p\right) \tag{7}$$

Combining Eqs. (1) and (7), and after algebraic simplification, the term (c_m-c_p) can be expressed in terms of c_p only as,

$$c_m - c_p = \frac{c_p}{\alpha c_p + \beta} \tag{8}$$

Substituting Eq. (8) in Eq. (6), the following nonlinear algebraic equation of c_p is obtained,

$$\frac{\beta v_w^0}{\alpha c_p+\beta} - k\ln\left[\frac{c_p}{\left(\alpha c_p+\beta\right)\left(c_0-c_p\right)}\right]=0 \tag{9}$$

where, $\beta = B/J_w^0$.

The mass transfer coefficient under laminar flow conditions is given by Leveque's equation,

$$Sh = \frac{kd_e}{D} = 1.86\left(ReSc\frac{d_e}{L}\right)^{\frac{1}{3}} \tag{10}$$

where, d_e is the hydraulic diameter of the flow channel. For a thin channel, the value of d_e is $4h$, where, h is the half height of the channel. The term $ReScd_e/L$ becomes $u_0d_e^2/DL$ after simplification. With a knowledge of the parameter values, i.e., D, a and B, Eq. (9) can be solved iteratively to obtain the value of c_p at a fixed set of operating conditions, i.e., ΔP,u_0 and c_0, and in turn, c_m from Eq. (8) and permeate flux from Eq. (7).

Numerical Solution

Since pretreated leather plant effluent consists of various salts at different concentration levels as well as some smaller sized organic materials, the three parameters, namely, diffusivity (D), osmotic coefficient (a), and solute permeability through membrane (B) are difficult to obtain. Hence, an optimization method is employed with an initial guess of these three parameters and minimizing the following error function to obtain the values of these parameters,

$$S = \sum_{i=1}^{N} \left(\frac{J^{\exp} - J^{calc}}{J^{\exp}} \right)^2 + \sum_{i=1}^{N} \left(\frac{c_p^{\exp} - c_p^{calc}}{c_p^{\exp}} \right)^2 \tag{11}$$

The above optimization process is applied both for NF and RO and the model parameters are evaluated for both the systems. BCPOL subroutine of IMSL library using unconstrained direct search algorithm is used for optimization and Newton-Raphson algorithm is employed for solution of Eq. (9).

EXPERIMENTAL

Effluent

Effluent is collected from the main drain of M/s Alison Tannery, Kolkata, India, which contains all the effluent from the "wet blue" process except the chrome tanning. The characterization of the effluent has been carried out and is presented in Table 1.

Chemicals Used

Potassium alum is used for the coagulation and is procured from the local market. All the chemicals, required for the determination of COD and BOD, are procured from Loba Chemie India. All chemicals are of analytical grade and are used without further treatment.

Nanofiltration of the Effluent

Membranes

Organic polyamide membranes of molecular weight cut off of 400 is used for nanofiltration. The NF membrane is selected to remove the organic materials first, so that the solid load on RO becomes less. A thin film composite polyamide membrane is used for reverse osmosis. All the membranes are procured from M/s, Genesis Membrane Sepratech Pvt. Ltd., Mumbai, India.

Table 1. Characterization of leather plant effluent

COD (mg/l)	BOD (mg/l)	pH	Conductivity (mS)	TDS (kg/m^3)	TS (kg/m^3)	Turbidity (NTU)	Total sulphides (mg/l)
4335	1800	3.39	138	92	116	157	5100

The permeabilities of the membrane are determined using distilled water and are estimated to be 3.25×10^{-11} m/Pa·s for NF and 7.52×10^{-12} m/Pa · s for the reverse osmosis membrane. The range of the operating pressure is 414 to 966 kPa for NF membrane and that for RO is 828 to 1380 kPa in order to determine their permeabilities. The nanofiltration membrane is charged and its isoelectric point is 2.9.

Membrane Filtration Cell

The clarified effluent is pumped by a high pressure reciprocating pump from the stainless steel feed tank to the cross flow cell with a rectangular channel. The effective length of the membrane is 37.3×10^{-2} m and the width is 5.2×10^{-2} m. The channel height is determined by the thickness of the rectangular teflon gasket and this height is 3.44×10^{-3} m. The retentate stream is recycled back to the feed tank. Because of recycling maximum increase in the feed concentration (in terms of total solids) is about 1% in the feed and hence, it is assumed that recycling does not influence the process. The pressure and the cross flow rate inside the membrane channel are independently set by operating the valves in the bypass line and that at the outlet of the membrane cell. Permeate samples are collected from the bottom of the cell and are analyzed for COD, BOD, TS (total solids), TDS (total dissolved solids), conductivity and pH. The schematic of the experimental set up is available elsewhere (18).

Operating Conditions

The operating pressures for NF are 414, 552, and 828 kPa and those for RO are 828, 1104, and 1242 kPa. The cross flow rates are 30 ($Re = 320$), 75 ($Re = 800$), and 120 l/h ($Re = 1280$). These cross flow rates correspond to the cross flow velocities, as, 0.05, 0.12, and 0.19 m/s, respectively. For RO runs, feed is generated by collecting the permeating solution through a NF membrane at 828 kPa and $Re = 1280$.

Procedure

Pretreatment

The effluent is kept in five 500 ml capacity beakers. The optimum coagulant is determined by adding 0.2 to 3 g/l alum to the effluent and measuring turbidity, BOD, COD, TS, and TDS after 30 minutes. Once the optimum coagulation dose is obtained, the supernatant of the gravity settled liquor is treated with the optimum alum dose. The gravity settlement is carried out in a 10 liter container. After coagulation, the sludge settles at the bottom and the supernatant is siphoned out. A fine nylon filter cloth is then used for further clarification of the collected supernatant. The clarified liquor is then treated by the membrane separation processes.

Nanofiltration and Reverse Osmosis

In the membrane-based experiments, each membrane is first compacted with distilled water using a higher pressure of the maximum operating pressure. The membrane permeability is estimated from the permeate flux versus pressure data, using distilled water. After that, the cell is charged with the pretreated effluent. The duration of the cross flow experiments are of one hour. The permeating solution is collected on a digital balance on a cumulative volume basis. From the slope of the cumulative volume versus time curve, the permeate flux is calculated. The permeate samples are collected at regular intervals for analysis.

Analysis

The conductivity, total dissolved solids (TDS), turbidity and pH of all samples (feed, permeate and retentate streams) are measured at room temperature using a deluxe water and soil analysis kit, model no 191E, manufactured by Toshniwal Instruments Ltd, India. Total solids (TS) of all the samples are measured by taking a known volume of sample in a petri dish and keeping in an oven maintained at $105 \pm 2°C$ till complete drying of the sample. COD and BOD are determined using standard techniques (19).

RESULTS AND DISCUSSION

Pretreatment of the Effluent

The supernatant of the pretreated effluent is taken out and various properties, e.g., pH, conductivity, TDS, TS, turbidity, BOD, and COD are measured. These properties of the alum treated effluent with the alum dose are tabulated in Table 2. It is clear from Table 2 that COD, BOD, turbidity, and TS decrease sharply with the increase in alum dose upto 1.0 g/l; but, the decrease is less for higher dosages of alum. Therefore, 1.0 g/l is considered as the optimum alum dose. Further, the pH at this level of alum concentration is almost neutral.

Table 2. Characterization of the clarified effluent after different alum doses

Alum dose (kg/m^3)	COD (mg/l)	BOD (mg/l)	Turbidity (NTU)	TS (kg/m^3)	pH	TDS (kg/m^3)
0.2	2970	1350	72.5	16.0	6.8	14.3
0.5	2880	1200	65.0	14.0	6.9	13.0
1.0	2280	850	43.8	14.0	7.7	12.8
2.0	2282	854	40.1	13.5	8.3	12.1
3.0	2284	856	38.2	13.5	8.6	11.9

After establishing the optimum alum dose, the effect of gravity settling is investigated. It is observed that the gravity settlement of 2 days results in a decrease in the COD from 4335 to 3768 mg/l. Therefore, the optimum alum dose is applied to the "gravity settled" solution and it results in a COD and BOD of 864 and 388 mg/l, respectively. The TS and the TDS are 14 and 13.7 g/l, respectively, after the sludge separation. The amount of sludge generated is 102 g/l after drying, which can be used as a fertilizer. The other properties are found to be in the same range of those with optimally alum treated solution without the gravity settling. Therefore, the effluent is first subjected to the gravity settling, followed by the alum treatment. The supernatant is then treated with the subsequent membrane filtration after a coarse filtration by a fine cloth.

Nanofiltration in the Cross Flow Mode

A detailed parametric study is conducted to observe the effects of the operating conditions on the permeate flux and the permeate quality.

Nanofiltration using 400 MWCO Membrane

A typical variation of the permeate flux profile with the operating time at $Re = 320$ for various operating pressures is shown in Fig. 2. It is clear from the figure that the permeate flux remains almost constant throughout the filtration run. Since, there is no indication of flux decline with time, unlike the unstirred batch cell experiments (under severe polarization conditions) (20), pore blocking and cake filtration are not the major flux decline mechanism. Therefore, the flux decline from pure water flux under cross flow conditions may be the osmotic pressure controlled. For all the operating conditions in NF, the same trend, i.e., constancy of permeate flux is observed almost from the beginning of the experiments. The variation of the steady state permeate flux with the transmembrane pressure is shown in Fig. 3. From the figure, it may be observed that the permeate flux increases almost linearly within the pressure range. For example, with increase in pressure from 414 to 828 kPa, the steady state flux increases from about 0.8×10^{-5} to $1.5 \times 10^{-5}\ \mathrm{m^3/m^2 \cdot s}$ (almost 100% increase). The effect of the flowrate on the permeate flux is also shown in Fig. 3, which shows that the flux is almost independent of the cross flow velocity within the experimental range considered herein. The variation of total dissolved solids in the permeate under various operating conditions are presented in Table 3. It is observed from Table 3 that the TDS values in the permeate decrease with the Reynolds number and the operating pressure. With an increase in the Reynolds number, the membrane surface concentration becomes less due to the forced convection, resulting in a lower permeation of solutes (TDS in this case) through the membrane. According to the solution-diffusion model,

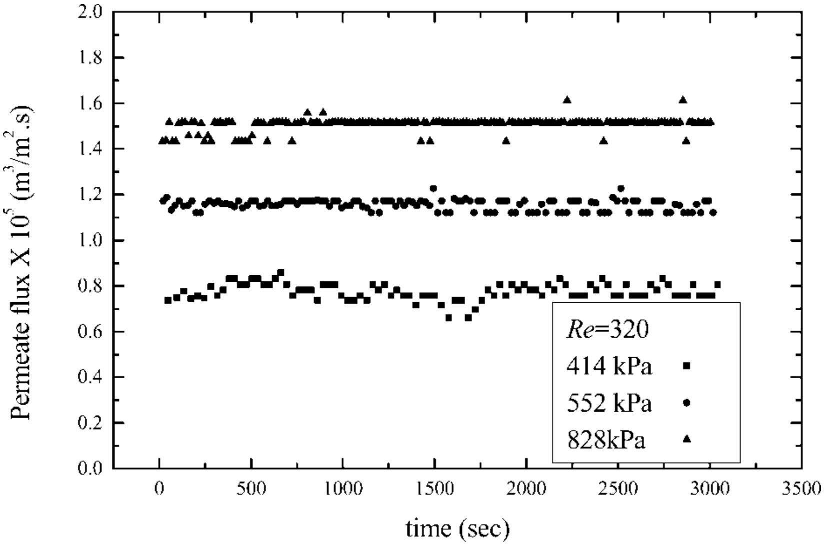

Figure 2. Profile of permeate flux decline during NF.

an increase in pressure results in the solvent to permeate more through the membrane, resulting in a lower solute concentration on the permeate side (21).

As discussed in the theory section, a combination of osmotic pressure and the solution diffusion model is used to estimate the effective osmotic pressure

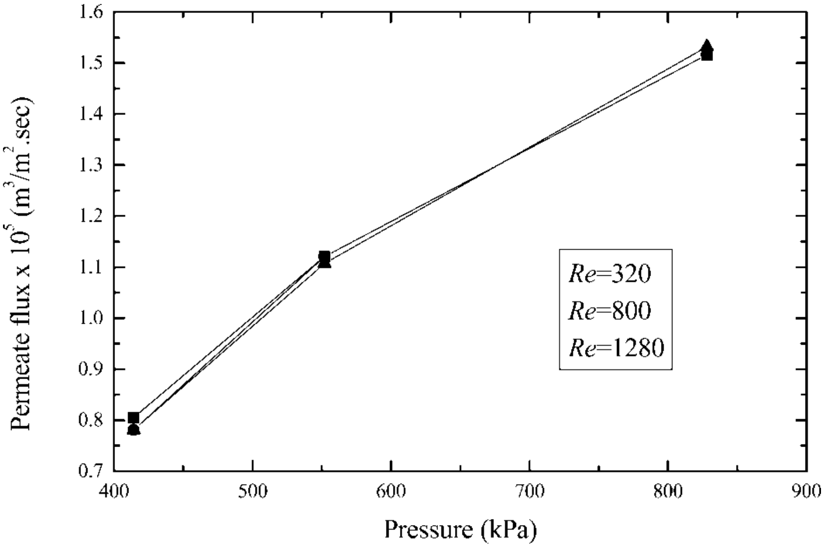

Figure 3. Variation of the steady state permeate flux with operating condition during NF.

Table 3. Variation of the steady state TDS with the operating conditions during NF

Operating pressure (kPa)	414			552			828		
Re	320	800	1280	320	800	1280	320	800	1280
TDS ($\mathrm{kg/m^3}$)	3.4	2.7	2.3	3.1	2.5	2.4	3.0	2.5	2.1

coefficient (a), solute diffusivity (D) and the solute permeability (B) through the membrane of this complex industrial effluent by optimizing the experimental flux and permeate the TDS concentration values. The optimized parameter values for NF are: $a = 7219$ Pa-m^3/kg, $D = 1.82 \times 10^{-9}$ m^2/s, $B = 2.17 \times 10^{-7}$ m/s. It may be observed that the effective osmotic pressure coefficient is one order of magnitude less than that of sodium chloride (about 80,000). This may be explained by the fact that in the feed of NF, apart from NaCl, other higher molecular weight salts, e.g., Na_2S, Na_2SO_4, etc. and some low molecular weight organic compounds are also present. Since, a is inversely proportional to the molecular weight of the solute, the value of the optimized a is one order of magnitude less than that of NaCl. The effective solute diffusivity is almost the same order of magnitude as that of NaCl (1.5×10^{-9} m^2/s). The slightly higher value indicates the presence of various salts at higher concentration (salt diffusivity increases slowly with concentration). At these optimized parameter combinations, the comparison between the experimental and calculated permeate flux and permeate concentration is presented in Figs. 4a and 4b, respectively. The figures show that the calculated values lie within $\pm 15\%$ of the experimental data. The extent of the polarization on the membrane surface is quantified in the form of the polarization modulus that is defined as $c_m - c_p/c_0 - c_p$. A variation of the polarization modulus with the operating pressure is presented in Fig. 5 for NF experiments. It is observed from the figure that the polarization modulus increases with pressure and decreases with the Reynolds number. Therefore, an optimum selection of the operating pressure and Reynolds number is required for the design of a membrane module.

The variation of steady state BOD and COD of permeate with pressure is shown in Fig. 6. From Fig. 6, it may be observed that the COD increases slowly with pressure due to increase in driving force. For example, at $Re = 320$, COD increases from 128 to 142 mg/l as pressure increases from 414 to 828 kPa. The effects of the Reynolds number are also evident in this case. At 828 kPa pressure, COD decreases from about 142 to 92 mg/l as the Reynolds number increases from 320 to 1280. It may be noted here that the permeate COD for all the operating conditions is well within the permissible limit, i.e., below 250 mg/l. The trends of BOD with pressure and flow rate are the same as that of the COD. A close examination of Fig. 6 reveals that apart from the operating conditions (414 kPa and $Re = 1280$) all BOD values are above 30 mg/L. In fact, the lowest BOD is at 30 mg/l, which is

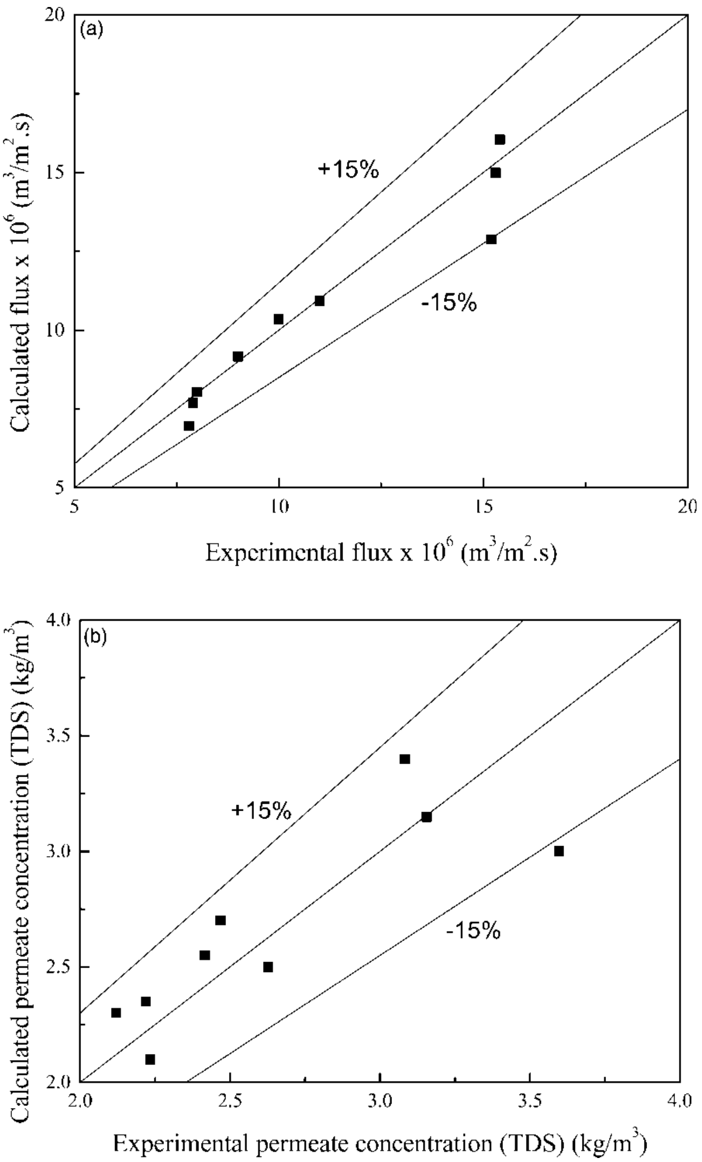

Figure 4. (a) Comparison between the experimental and calculated flux during NFb. (b) Comparison between the experimental and calculated permeate TDS concentration during NF.

the permissible limit. Therefore, although the permeate COD values of NF are within the permissible limit but it is desirable to bring down the BOD below the permissible limit. Therefore, one more filtration step using RO of the permeating solution generated from NF is required.

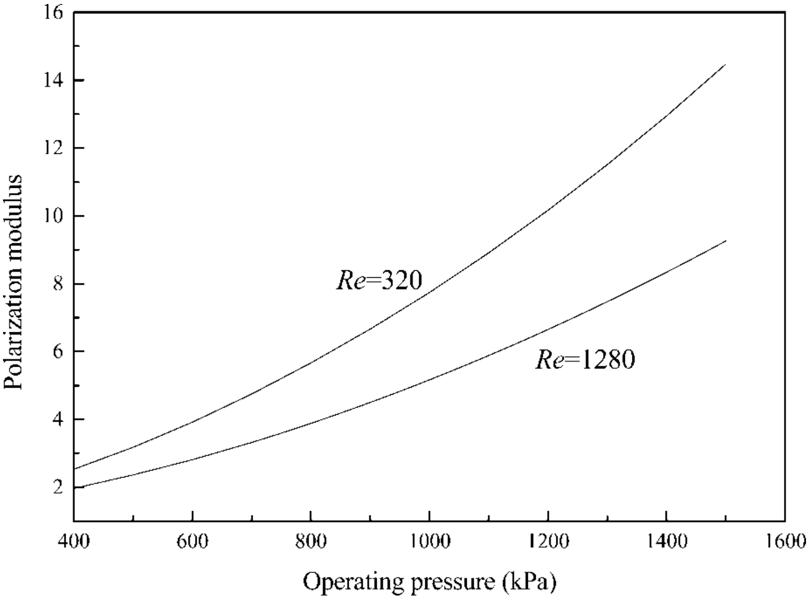

Figure 5. Variation of polarization modulus during NF.

Nanofiltration Followed by Reverse Osmosis

Variation of the permeate flux with the time of filtration at a typical Reynolds number ($Re = 320$) and different operating pressure is shown in Fig. 7. The

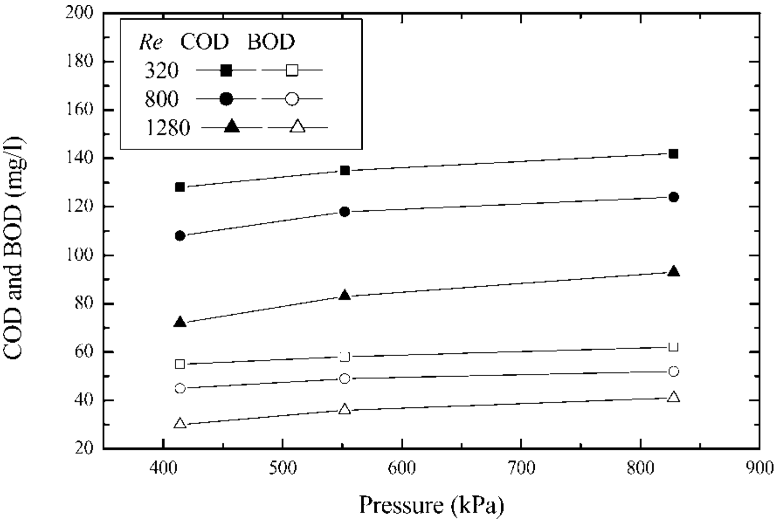

Figure 6. Variation of COD and BOD with operating conditions during NF.

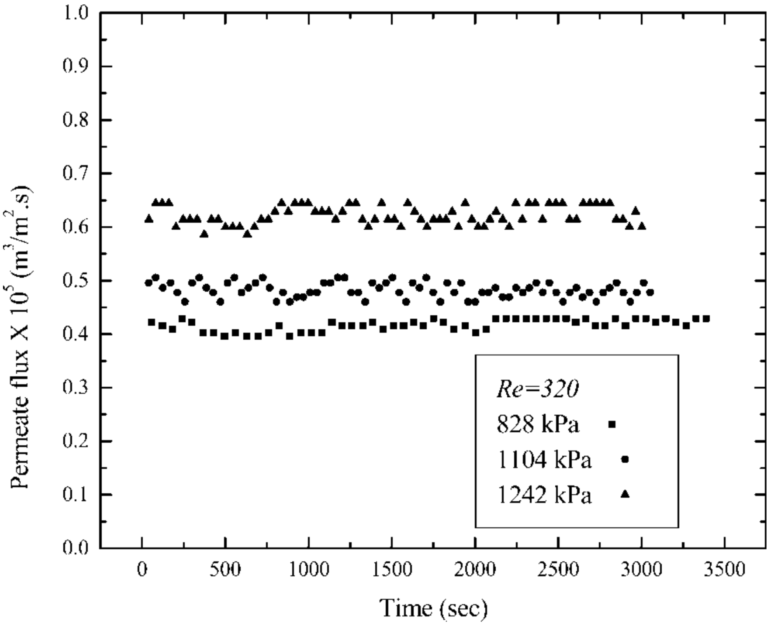

Figure 7. Permeate flux decline profile in RO.

figure shows that the permeate flux is almost time independent from the beginning of the experiments. This indicates that osmotic pressure is responsible for flux decline (from water flux) in a cross flow set up compared to pore blocking and cake filtration which are the dominant mechanism in batch cell experiments (20).

The variation of the steady state permeate flux with the operating pressure is shown in Fig. 8 for various Reynolds numbers. The effect of pressure is significant and the steady state flux increases from 4.2 to 6×10^{-6} m^3/m^2 s as the pressure increases from 828 to 1242 kPa. The effect of the cross flow rate (in terms of Reynolds number) is also shown in Fig. 8 and this effect is marginal within the range of Reynolds numbers in this study.

Since most of the organics are retained and almost all of the salts permeate in the NF stage, the feed for reverse osmosis mainly constitutes of inorganic salts. Keeping this in mind, the effective solute diffusivity is assumed to be that of NaCl and the other two parameters, i.e., effective osmotic pressure coefficient (a) and solute permeability through the membrane (B) are optimized as discussed in section 2. The optimized values of the parameters for RO are: $a = 1.0 \times 10^5$ Pa-m^3/kg and $B = 7.73 \times 10^{-7}$ m/s. It may be observed that the optimized value of the osmotic coefficient is really very close to that of pure sodium chloride, i.e., about 80,000. With these values of the parameters, the comparison between the calculated and the experimental permeate flux and permeate concentration

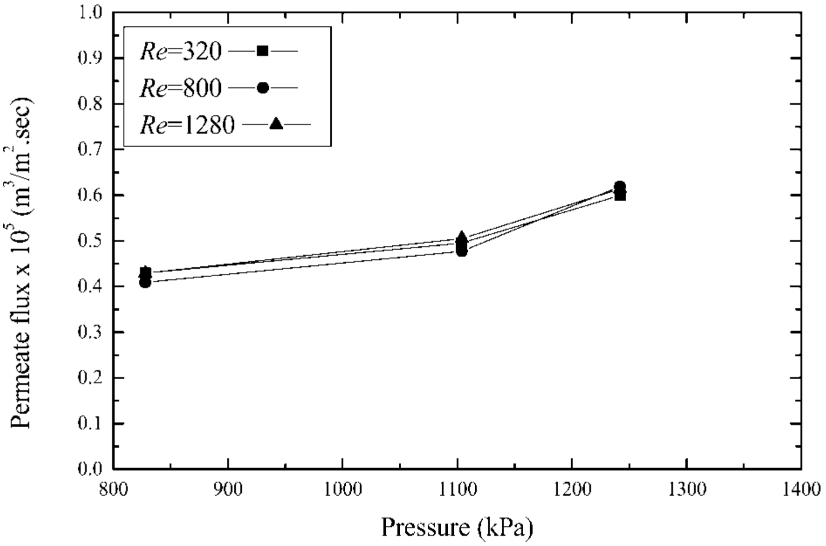

Figure 8. Variation of steady state permeate flux with operating conditions during RO.

values are plotted in Figs. 9a and 9b, respectively. From the figures, it is seen that the calculated values are well within ± 15% of the experimental data. The polarization modulus is also plotted for RO, in Fig.10. It is observed that the polarization modulus increases with the operating pressure and decreases with the Reynolds number, as expected. The variation of TDS with pressure for different Reynolds numbers is presented in Table 4.

Variations of COD and BOD with pressure for various Reynolds numbers are shown in Fig. 11. From Fig. 11, it may be observed that although the COD increases slightly with pressure, but all the values are well within the permissible limit. All the BOD values are less than the permissible values except that at the $Re = 320$. The COD and BOD values decrease with the Reynolds number significantly. For example, at 1242 kPa pressure, COD decreases from about 90 to 38 mg/l; whereas, BOD decreases from 40 to 20 mg/l, when the Reynolds number increases from 320 to 1280. Therefore, 1242 kPa pressure and $Re = 1280$ give the highest permeate flux and lowest BOD and COD values (well under the specified limits).

Comparison of the Performance of Exclusive NF and NF Followed by RO

The comparative performance data of NF and NF followed by RO is shown in Table 5. The operating pressures are 828 kPa and 1242 kPa for NF and RO, respectively and $Re = 1280$. It may be observed from Table 5 that COD in both the processes are within the permissible limit. BOD after the NF

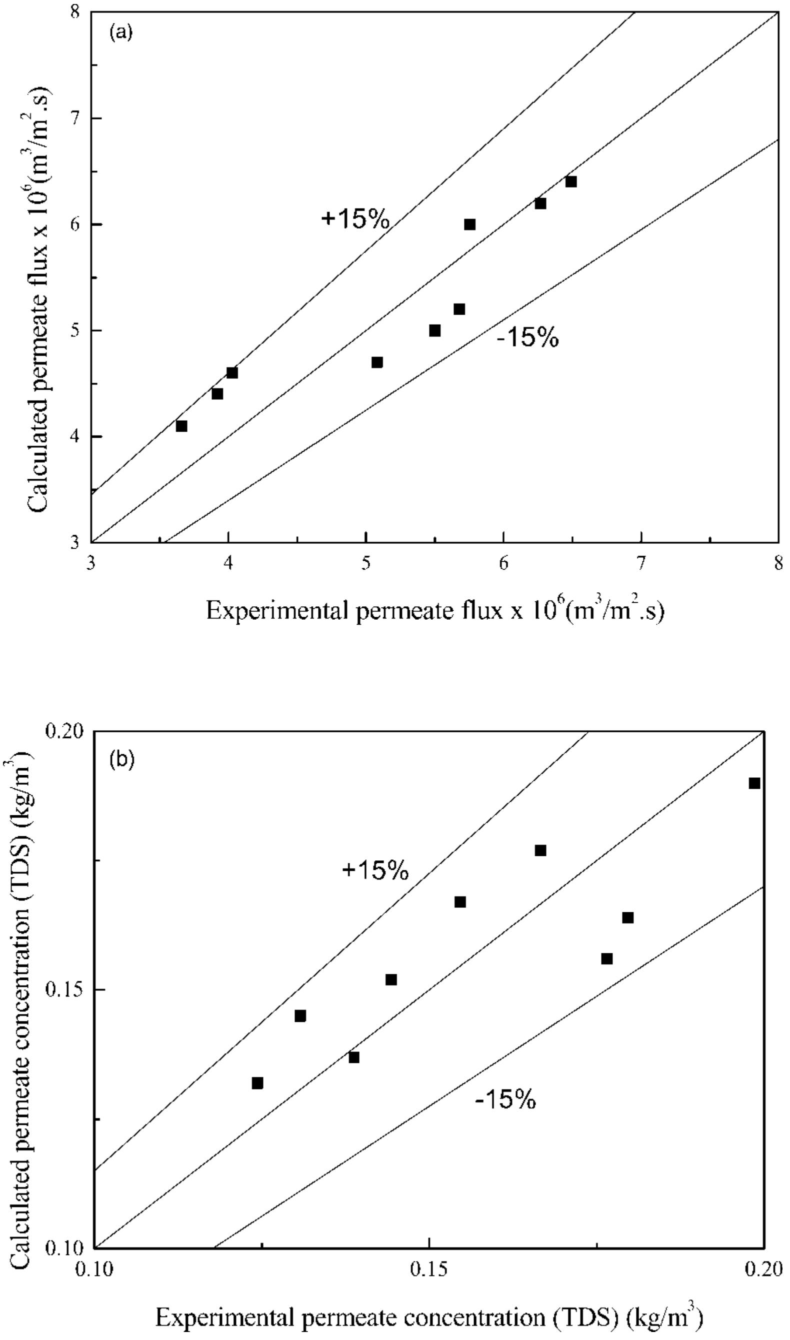

Figure 9. (a) Comparison between the experimental and calculated flux during RO. (b) Comparison between the experimental and calculated permeate concentration (TDS) during RO.

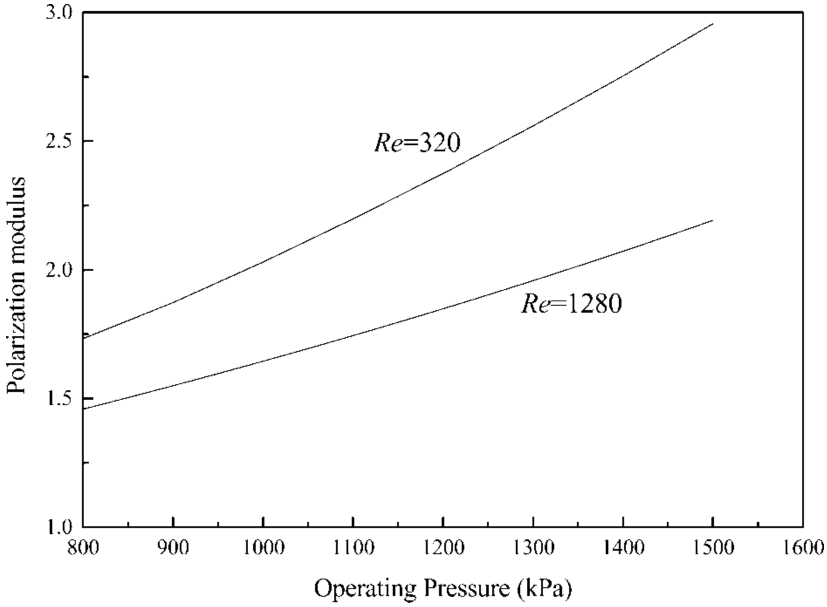

Figure 10. Variation of polarization modulus during RO.

process is beyond the permissible limit. On the other hand, the permeating solution of RO has a BOD well within the permissible limit. In order to meet the permissible limit of the treated effluent, one has to sacrifice the permeate flux. From Table 5, it is clear that the permeate flux is $1.53 \times 10^{-5}\ m^3/m^2 \cdot s$ after the NF and the flux is about $0.65 \times 10^{-5}\ m^3/m^2 \cdot s$ after RO. Therefore, the clarified leather effluent may be safely treated using NF followed by RO so that the COD and BOD of the permeate remain within the permissible limit and the treated stream can be discharged or reused.

CONCLUSION

All the effluent coming out from various process streams of a leather plant, except chrome tanning, are treated with a series of pretreatment processes,

Table 4. Variation of the steady state TDS with the operating conditions during RO using the permeate from NF as feed

Operating pressure (kPa)		828			1104			1242	
Re	320	800	1280	320	800	1280	320	800	1280
TDS (kg/m^3)	0.20	0.18	0.16	0.18	0.17	0.16	0.16	0.13	0.12

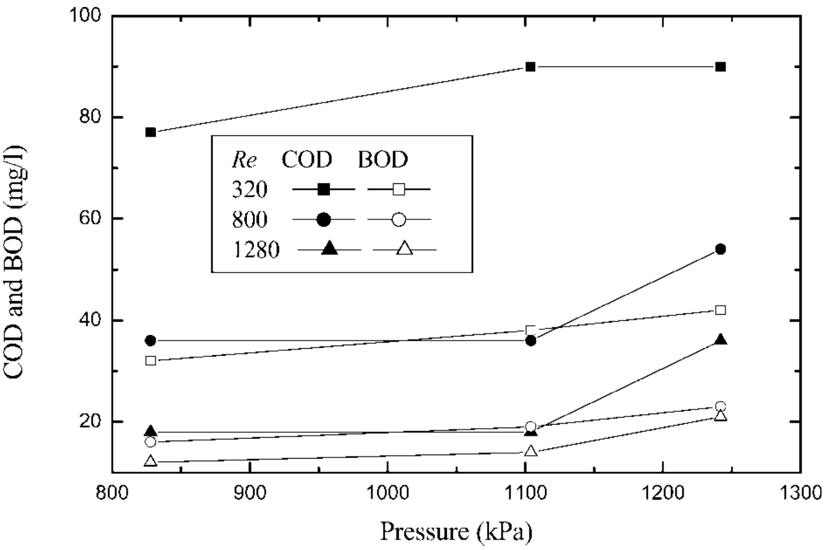

Figure 11. Variation of COD and BOD with operating conditions during RO.

namely gravity settling, coagulation, and cloth filtration. The optimum alum dose for coagulation is found to be 1.0 g/l. The supernatant is then subjected to NF followed by RO. A systematic parametric study is conducted to observe the effects of the operating variables on the permeate flux and quality; both for NF and RO under cross flow mode of operation. The suitable operating pressure for NF is 828 kPa and that for RO is 1242 kPa. $Re = 1280$ is found suitable for both the cases. The permeate BOD and COD of the treated effluent is found to be well within the permissible limit (applicable in India). A combination of the osmotic pressure and the solution diffusion model is used to quantify the flux decline. A method is outlined to estimate the effective osmotic pressure coefficient, the solute diffusivity, and the solute permeability through the membrane. For NF, the

Table 5. Comparison of performance between NF and NF followed by RO; operating conditions are 828 kP for NF and 1242 kPa for NF followed by RO at $Re = 1280$

BOD of the effluent treated by NF (mg/l)	41
COD of the effluent treated by NF (mg/l)	93
BOD of effluent treated by NF followed by RO (mg/l)	21
COD of effluent treated by NF followed by RO (mg/l)	36
Permissible BOD of effluent in India (mg/l)	30
Permissible COD of effluent in India (mg/l)	250
Permeate flux after NF ($m^3/m^2 \cdot s$)	1.53×10^{-5}
Permeate flux after NF followed by RO ($m^3/m^2 \cdot s$)	0.65×10^{-5}

value of the osmotic pressure coefficient and effective diffusivity reveal that the feed of NF contains mostly inorganic salts with some organic materials as well. These values for RO show that the feed of RO is mainly inorganic salts. The calculated permeate flux and permeate TDS concentration values are within ± 15% of the experimental data.

NOMENCLATURE

a	osmotic pressure coefficient ($\text{Pa} \cdot \text{m}^3/\text{kg}$)
B	solute permeability through the membrane (m/s)
c	concentration (kg/m^3)
c_m	membrane surface concentration (kg/m^3)
c_p	permeate concentration (kg/m^3)
c_p^{exp}	experimental permeate concentration (kg/m^3)
c_p^{calc}	calculated permeate concentration (kg/m^3)
c_0	feed concentration (kg/m^3)
d_e	hydraulic diameter (m)
D	effective solute diffusivity (m^2/s)
h	channel half height (m)
k	mass transfer coefficient (m/s)
L	channel length (m)
L_p	membrane permeability ($\text{m}/\text{Pa} \cdot \text{s}$)
Re	Reynolds number ($\rho\, u_0\, d_e/\mu$)
Sh	Sherwood number ($\text{kd}_\text{e}/\text{D}$)
Sc	Schmidt number ($\mu/\rho D$)
u_o	average velocity (m/s)
J	permeate flux ($\text{m}^3/\text{m}^2 \cdot \text{s}$)
J_w^0	pure water flux ($\text{m}^3/\text{m}^2 \cdot \text{s}$)
J^{exp}	experimental permeate flux ($\text{m}^3/\text{m}^2 \cdot \text{s}$)
J^{calc}	calculated permeate flux ($\text{m}^3/\text{m}^2 \cdot \text{s}$)

Greek Symbols

ΔP	transmembrane pressure drop (Pa)
Δ_π	osmotic pressure difference (Pa)
π_m	osmotic pressure at the membrane surface (Pa)
π_p	osmotic pressure at the permeate side (Pa)

ACKNOWLEDGEMENT

One of the authors (PKB) acknowledges the funding received from the Indo-French Center for the Promotion of Advanced Research (IFCPAR) in partial support to this work. SD acknowledges the financial support provided by IIT

Kharagpur as the submission project under Manufacturing and System Engineering (IIT/SRIC/MSE/2003-2004/99).

REFERENCES

1. Dutta, S.S. (1999) *An Introduction to the Principles of Leather Manufacture*; Indian Leather Technologists' Association: Calcutta.
2. Rao, J.R., Chandrababu, N.K., Muralidharan, C., Nair, B.U., Rao, P.G., and Ramasamy, T. (2003) Recouping the wastewater: a way forward for cleaner leather processing. *J. Cleaner Prod.*, 11: 591–599.
3. More, S.V., John, S., Rao, B.S., Nair, B.U., and Laxman, R.S. (2001) Chromium removal and reduction in COD of tannery effluents by actinomyates. *Indian J. Environ. Health.*, 43 (3): 108–113.
4. Marcucci, M., Ciardelli, G., Matteucci, A., Ranieri, L., and Russo, M. (2002) Experimental campaigns on textile wastewater for reuse by means of different membrane processes. *Desalination*, 149: 137–143.
5. Afonso, M.D. and Pinho, M.N.D. (1991) Membrane separation processes in the pulp and paper industry. *Desalination*, 85 (1): 53–58.
6. Brans, G., Schroen, C.G.P.H., van der Sman, R.G.M., and Boom, R.M. (2004) Membrane fractionation of milk: state of the art and challenges. *J. Membrane Sci.*, 243: 263–272.
7. Jönsson, A.S. and Trägårdh, G. (1990) Ultrafiltration applications. *Desalination*, 77: 135–179.
8. Cassano, A., Molinari, R., Romano, M., and Drioli, E. (2001) Treatment of aqueous effluents of the leather industry by membrane processes: A review. *J. Membrane Sci.*, 181: 111–126.
9. Taleb Ahmed, M., Taha, S., Chaabane, T., BenFarès, N., Brahimi, A., Maachi, R., and Dorange, G. (2005) Treatment of sulfides in tannery bath by nanofiltration. *Desalination*, 185: 269–274.
10. Cassano, A., Drioli, E., and Molinari, R. (1998) Integration of ultrafiltration into unhairing and degreasing operations. *J. Soc. Leather Technologists Chemists*, 82: 130–135.
11. Cassano, A., Criscuoli, A., Drioli, E., and Molinari, R. (1999) Clean operations in the tanning industry: aqueous degreasing coupled to ultrafiltration: experimental and theretical analysis. *Clean Product Processes*, 1 (4): 257–267.
12. Cassano, A., Drioli, E., Molinari, R., and Bertolutti, C. (1996) Quality improvement of recycled chromium in the tanning operation by membrane processes. *Desalination*, 108: 193–203.
13. Scholz, W. and Lucas, M. (2003) Techno-economic evaluation of membrane filtration for the recovery and reuse of tanning chemicals. *Water Res.*, 37: 1859–1867.
14. Cassano, A., Adzet, J., Molirani, R., Buonomenna, M.G., Roig, J., and Drioli, E. (2003) Membrane treatment by nanofiltration of exhausted vegetable tanning liquors from the leather industry. *Water Res.*, 37 (10): 2426–2434.
15. Saalan, H.F., Sorour, M.H., and Tewfik, S.K. (2001) Simulation and optimization of a membrane system for chromium recovery from tanning wastes. *Desalination*, 141: 315–324.
16. Padilla, A.P. and Tavani, E.L. (1999) Treatment of an industrial effluent by reverse osmosis. *Desalination*, 126: 219–226.

17. Viero, A.F., Mazzarollo, A.C.R., Wada, W., and Tessaro, I.C. (2002) Removal of hardness and COD from retanning treated effluent by membrane process. *Desalination*, 149: 145–149.
18. Purkait, M.K., DasGupta, S., and De, S. (2005) Micellar enhanced ultrafiltration of phenolic derivatives from their mixture. *J. Colloid & Interf. Sci.*, 285: 395–402.
19. Trivedi, R.K. and Goel, P.K. (1986) *Chemical and Biological Methods for Water Pollution Studies*, 2nd ed.; Environmental Publication: Aligarh.
20. Purkait, M.K., Bhattacharya, P.K., and De, S. (2005) Membrane filtration of leather plant effluent: Flux decline mechanism. *J. Membrane Sci.*, 258: 85–96.